Performance Study of Variable-Rate Modulation for Underwater Communications based on Experimental Data

Beatrice Tomasi*, Laura Toni‡, Paolo Casari*, Lorenzo Rossi‡, Michele Zorzi*

*Department of Information Engineering, University of Padova, Italy — {tomasibe, casarip, zorzi}@dei.unipd.it

‡Italian Institute of Technology (IIT), Genova, Italy — {laura.toni, lorenzo.rossi}@iit.it

***Abstract*—In this paper, we present an analysis of the performance of a variable-rate adaptive modulation system based on instantaneous SNR information. The SNR traces we consider are part of the SubNet'09 experimental dataset, and have been derived by processing an hyperbolic frequency-modulated signal in the 9–14 kHz band. We start by deriving the high level behavior of the channel in terms of the statistics of channel fading effects, which are found to be well modeled by a Nakagami–m distribution, where the parameter m is estimated over a whole experiment or over smaller time windows throughout the experiment, depending on the variability of the SNR. The statistics of the channel behavior are then used to derive the performance of a variable-rate modulation scheme switching between five different constellations; the cases of both instantaneous and outdated channel knowledge are considered.**

Analytical results are compared to simulations to show that the Nakagami-m distribution can satisfactorily capture the statistics of the channel, provided that the estimation of the m parameter, as well as of the correlation of the SNR process, is repeated in case of macroscopic channel variations.

I. Introduction and Related Work

The great deal of work currently being devoted to the design of reprogrammable underwater acoustic modem hardware (e.g., see [1], [2]) is paving the way for the practical implementation of more efficient techniques to improve the effectiveness of digital signaling through underwater channels. In fact, underwater communications face time-varying propagation, where the variation in time exhibits a twofold, fast and slow nature [3]. Especially in shallow water channels, the environment gives rise to time-varying multipath patterns even when the transmitter and receiver are fixed. Surface waves, currents, internal waves [4], as well as day/night cycles all contribute to changing the way the signal is received across underwater links.

Significant efforts have been spent to characterize the underwater channel changes at least from a high level point of view: while several studies assume that the channel can be described by a Rayleigh process [5], [6], some other works challenge this assumption, and make use of Rayleigh statistics for the amplitude of acoustic signal replicas reaching the receiver, or alternatively resort to Rice models, which fit better in some cases [7]. Alternatively, some works assume an iso-velocity environment, and simulate channel changes by considering the superposition of all channel eigenrays as modulated by a Rayleigh process [8]. In any event, the estimated or derived statistics of the channel can be exploited in order to improve the performance of underwater communications. In particular, some system parameters, from transmit power to the type of digital modulation or coding scheme in use, could be dynamically adapted to varying channel conditions.

In this paper, we focus on adaptive modulation (AM) schemes, which tune the constellation size of the used modulation, depending on the available information about the channel state, e.g., as perceived by the transmitter or as fed back by the receiver. The purpose of AM is two-fold: to achieve higher spectral efficiency (by using more efficient modulations whenever the channel so allows) and to reduce the chance of outage events (by avoiding the use of complex schemes when the channel cannot support them). While AM is a well established technique for link adaptation in terrestrial radio networks [9]–[12], it has received comparatively much less attention in underwater acoustic networks. However, a few works do propose the use of AM. In particular, [13] focuses on variable-rate Mary Frequency-Shift Keying (FSK) modulations, where the proper rate is chosen based on a preliminary exchange of control packets for SNR estimation. The use of AM is also generally documented as part of LinkQuest's modems firmware [14], although no further details on the adaptation algorithm are provided. Adaptive modulation and coding has also been analyzed in [15], where the authors post-process data collected during the AUVfest 2007 campaign. A transmit array of 10 elements and a receive array of 8 elements were deployed in the Gulf of Mexico; different modulation (from Binary Phase-Shift Keying (BPSK) to multi-level PSK) and turbo coding rates (from $7/8$ down to $1/3$) were employed to modulate the subcarriers of a multitone transmit signal in both a Single Input Single Output (SISO) and a Multiple Input Multiple Output (MIMO) configuration. The overlooking of AM can be at least partially explained by the difficulty of implementing such schemes in real-time systems today. However, the next generations of underwater devices (especially the aforementioned projects embedding

reprogrammability and allowing for user-defined waveforms and processing algorithms to be implemented in the modem's firmware) will be likely able to support real-time variable-rate modulation.

Depending on the rate at which adaptation is performed, we distinguish between Fast AM (FAM) which tracks fast channel changes, and thus achieves better spectral efficiency at the price of frequent channel estimation or feedback from the receiver, and Slow AM (SAM), which adapts to the average of the SNR process, thus requiring less processing and feedback. In the present paper, we assume that the channel SNR process is updated once for every received packet, and that the corresponding SNR value is fed back to the transmitter so that the adaptation of the modulation scheme can be performed prior to the subsequent transmission. As we will detail in the next section, the transmissions of our dataset are sufficiently spaced to make a per-packet modulation update process feasible. However, in order to simulate a less ideal case where greater delay affects the feedback from the receiver, we also consider the availability of only outdated channel estimates. In any event, the system considers instantaneous (instead of average) SNR samples to be fed back to the transmitter, and is thus a FAM system in light of the previous definitions. Starting from Signal-to-Noise Ratio (SNR) traces, we discuss their fitting using Rayleigh as well as Nakagami-m distributions, and use the models to obtain the performance of simple BPSK as well as more complex Mary quadrature amplitude modulation (M-QAM) schemes with square constellation. We note that perfect Channel State Information (CSI) at the transmitter is assumed here: given that the only information required to run the AM scheme is the SNR of the current transmission, this assumption is reasonable.

In the following sections, we give the details of our approach by describing the channel model, the set of modulation schemes the system can choose from, the source of our channel traces, as well as our analysis and simulation results. We finally conclude our paper in Section V.

II. System model and performance analysis

In this paper, we consider an adaptive modulation system using BPSK and M-QAM constellations signaling over Nakagami-m fading channels. In particular, we assume that a finite set of $J+1$ modulation schemes can be chosen, each having a different constellation size $\{M_0, M_1, \ldots, M_J\}$, and leading to a different probability of error as a function of the receive SNR and a different spectral efficiency, in terms of bits transmitted per channel use. For the purposes of the present study, let $M \in \{2, 4, 16, 64, 256\}$:[1] therefore $J = 4$. While we refer the reader to [9] for details on variable-rate adaptive M-QAM modulation under the ideal CSI assumption, we remark here that the rationale behind the adaptation of the modulation signaling is to exploit the changes in the channel propagation gain to the system's advantage, i.e., by pushing a larger number of bits per symbol through a constellation with a higher number of levels when the SNR is favorable, while backing off to more robust constellations (such as BPSK's or QPSK's) whenever the SNR drops below an acceptable value for higher-order modulations. To this end, a straightforward solution (which we consider in this paper) is to choose the modulation for the current transmission in an opportunistic fashion, i.e., by choosing the modulation j, with M_j levels, whenever the measured SNR γ falls within a prescribed interval of the form $[\gamma_j^*, \gamma_{j+1}^*)$. The thresholds γ_j^* and γ_{j+1}^* are chosen so that the SNR is at least as high as required to ensure a prescribed performance level with modulation j (e.g., a bit error rate (BER) of no more than a desired level P_{b}^*), yet insufficient to achieve the same performance using the higher spectral efficiency modulation $j+1$. Some hysteresis may be built into the switching scheme to prevent continual level changing [17], but this solution, though practical, does not yield additional insight to the analysis we carry out in the following, and is therefore not considered here. The spectral efficiency achieved by choosing modulation j is then $\log_2 M_j$ bits per channel use, $j = 0, \ldots, J$.

From a practical standpoint, given a transmitter-receiver pair, the receiver is assumed to provide a measure of the SNR γ to the transmitter, which will then take the highest j such that the modulation with M_j levels has a bit error rate (BER) $P_{\mathrm{b}}(\gamma) < P_{\mathrm{b}}^*$, where P_b^* is some desirable value.[2] For BPSK, as well as for M-QAM the exact formula of the BER is given in (1) [18], where $Q(x) \triangleq \int_x^\infty e^{-t^2/2}\,\mathrm{d}t/\sqrt{2\pi}$ is the Gaussian-Q function. Whenever the SNR falls below the value required to guarantee a BER of no more than P_{b}^* to the most robust modulation with $M_0 = 2$ levels, the system is said to be in outage. However, note that such definition of outage is only valid under an instantaneous channel knowledge assumption. We will relax this later by accounting for outdated knowledge, and therefore extend the concept of outage correspondingly.

For now, assume that the SNR, ideally estimated at the

[1] We note that these modulations are standard in digital video transmission, e.g., 4- to 64-QAM are used in the European Telecommunications Standards Institute (ETSI)'s DVB-T standard, whereas the 16- to 256-QAM schemes are adopted in the DVB-C standard [16].

[2] In the following evaluation, P_b^* will be fixed to 10^{-2}.

$$P_{\mathrm{b}}^{(j)}(\gamma) = \begin{cases} Q\left(\sqrt{2\gamma}\right), & j = 0 \\ \dfrac{2/\sqrt{M_j}}{\log_2(\sqrt{M_j})} \displaystyle\sum_{h=1}^{\log_2(\sqrt{M_j})} \sum_{i=0}^{(1-2^{-h})\sqrt{M_j}-1} (-1)^{\left\lfloor \frac{i2^{h-1}}{\sqrt{M_j}} \right\rfloor} \left(2^{h-1} - \left\lfloor \frac{i2^{h-1}}{\sqrt{M_j}} + \frac{1}{2} \right\rfloor\right) Q\left((2i+1)\sqrt{\frac{3\gamma}{(M_j-1)}}\right), & j > 0 \end{cases} \tag{1}$$

receiver, is sent back to the transmitter on an error-free delayed channel. Also, recall that the channel fading effects are modeled by a Nakagami-m process. Let E_s denote the symbol energy (averaged over the distribution of fading), $N_0/2$ the two-sided power spectral density of the additive white Gaussian noise process at the receiver, and h the fading gain, assumed in this paper to have a Nakagami-m distribution. Because the instantaneous SNR can be written as $\gamma = |h|^2 E_\mathrm{s}/N_0$ its probability density function (pdf) $f_\gamma(\gamma)$ and its cumulative distribution function (cdf) $F_\gamma(\gamma)$ are respectively given by [19, pp. 21–24]

$$f_\gamma(\gamma) = \frac{m^m \gamma^{m-1}}{\overline{\gamma}^m \Gamma(m)} \exp\left(-\frac{m\gamma}{\overline{\gamma}}\right), \quad (2)$$

$$F_\gamma(\gamma) = 1 - \frac{\Gamma\left(m, \frac{m\gamma}{\overline{\gamma}}\right)}{\Gamma(m)}, \quad (3)$$

for $\gamma \geq 0$, where $\Gamma(\cdot)$ is the Gamma function, $\overline{\gamma} = \mathbb{E}\left[|h|^2\right] E_\mathrm{s}/N_0$, is the mean SNR, and m is the Nakagami-m fading parameter, which ranges from $1/2$ to $+\infty$.

For a given maximum target BER, typical performance metrics for adaptive modulation systems are the average spectral efficiency (SE), defined as the average number of bits per channel use allowed by the adaptation scheme, and the bit error outage (BEO), defined as the probability that the system cannot satisfy the prescribed performance in terms of bit error rate. We consider both metrics in the following, and provide their analytical expressions in the presence of both instantaneous and outdated channel knowledge at the transmitter.

A. Instantaneous channel knowledge

Ideal adaptive modulation systems are said to be in outage whenever the SNR makes the most robust modulation M_0 achieve a bit error probability (BEP) worse than P_b^*. When ideal CSI (perfect channel estimation and instantaneous channel knowledge) is available at the transmitter, the BEO can be evaluated as the probability of experiencing an SNR level lower than the minimum threshold γ_0^*:

$$P_\mathrm{o}(P_\mathrm{b}^*) = \mathbb{P}\left\{P_\mathrm{b}^{(0)}(\gamma) > P_\mathrm{b}^*\right\} = F_\gamma\left(\gamma_0^*\right). \quad (4)$$

The average SE can be expressed in terms of the number of bits per symbol in each modulation, averaged over the probability of choosing that modulation:

$$\begin{aligned}\eta &= \sum_{j=0}^{J-1} \tilde{M}_j \, \mathbb{P}\left\{\gamma_j^* < \gamma \leq \gamma_{j+1}^*\right\} + \tilde{M}_J \, \mathbb{P}\left\{\gamma_J^* < \gamma\right\} \\ &= \sum_{j=0}^{J-1} \tilde{M}_j \left[F_\gamma(\gamma_{j+1}^*) - F_\gamma(\gamma_j^*)\right] + \tilde{M}_J \left[1 - F_\gamma(\gamma_J^*)\right], \quad (5)\end{aligned}$$

where $\tilde{M}_j = \log_2 M_j$. We also define the throughput of the system, denoted as G in the following, by taking the product of the spectral efficiency of either modulation and the related probability of correct bit reception, averaged over the values of the SNR for which that modulation is chosen. We have

$$G = \sum_{j=0}^{J} \tilde{M}_j \int_{\gamma_j^*}^{\gamma_{j+1}^*} \left[1 - P_\mathrm{b}^{(j)}(\gamma)\right] f_\gamma(\gamma) \, \mathrm{d}\gamma, \quad (6)$$

where we let $\gamma_{J+1}^* = +\infty$.[3]

B. Outdated CSI

We now evaluate the effect of delayed channel knowledge on the system performance. To this end, we assume that the information about the value of the SNR γ, estimated by the receiver at a given time t, will be available at the transmitter only after a delay τ, i.e., at time $t+\tau$. Therefore, the opportunistic choice of the constellation size will still be based on the value of γ, but when such a constellation will be used, i.e., at time $t+\tau$, the SNR will have evolved to a different value $\gamma_\tau = |h_\tau|^2 E_s/N_0$ [4]. At this point, if $\gamma < \gamma_\tau$, the SNR is underestimated and, compared to the instantaneous knowledge case, a too conservative constellation size might be chosen for transmission. On the contrary, when $\gamma > \gamma_\tau$, the SNR is overestimated, and the chosen modulation level might not meet the prescribed BER requirements. In other words, although $\gamma \in [\gamma_j^*, \gamma_{j+1}^*)$, leading to the choice of modulation j, γ_τ might be such that $P_\mathrm{b}^{(j)}(\gamma_\tau) > P_\mathrm{b}^*$. In the latter case, the system is also in outage. In particular, an outage event occurs if $\gamma < \gamma_0^*$ or $\gamma \geq \gamma_0^*$, $\gamma \in [\gamma_j^*, \gamma_{j+1}^*)$ (hence, modulation j is chosen), but $\gamma_\tau < \gamma_j^*$. Then, the BEO can be written as

$$P_\mathrm{o} = F_\gamma\left(\gamma_0^*\right) + \sum_{j=0}^{J} P_{\mathrm{o}|j}, \quad (7)$$

where $P_{\mathrm{o}|j}$ denotes the joint probability that the current SNR is not sufficient to withstand the requirements of modulation j, and is found by integrating the distribution of γ_τ over $[0, \gamma_j^*)$ (i.e., where modulation j is in outage) and that γ was sufficient to enable the use of modulation j:

$$P_{\mathrm{o}|j} = \int_{\gamma_i^*}^{\gamma_{i+1}^*} \int_0^{\gamma_j^*} f_{\gamma_\tau|\gamma}\left(\gamma_\tau\right) f_\gamma(\gamma) \, \mathrm{d}\gamma_\tau \, \mathrm{d}\gamma, \quad (8)$$

where we let $\gamma_{J+1}^* = +\infty$, and $f_{\gamma_\tau|\gamma}(\gamma_\tau)$ is the pdf of γ_τ conditioned on γ. This distribution can be found as [20]

$$\begin{aligned}f_{\gamma_\tau|\gamma}\left(\gamma_\tau\right) = &\frac{m}{(1-\rho_\tau)\overline{\gamma}} \left(\frac{\gamma_\tau}{\rho_\tau \gamma}\right)^{(m-1)/2} \\ &\times I_{m-1}\left(\frac{2m\sqrt{\rho_\tau \gamma \gamma_\tau}}{(1-\rho_\tau)\overline{\gamma}}\right) \exp\left(\frac{m(\rho_\tau \gamma + \gamma_\tau)}{(1-\rho_\tau)\overline{\gamma}}\right), \quad (9)\end{aligned}$$

where $I_{m-1}(\cdot)$ is the modified Bessel function of the first kind and order $m-1$ [21], and ρ_τ is the correlation factor between

[3] We note that the analysis is conceptually equivalent if we consider the packet error probability instead of the bit error probability.

[4] In the following we assume that the channel is stationary and thus assume $t = 0$ with no loss of generality. From a practical standpoint, this translates into considering a portion of the experiment within a limited time window, during which the channel exhibits an approximately stationary behavior.

the SNR process and its τ-lagged version, which is estimated as

$$\rho_\tau = \frac{\sum_{t=0}^{N-1}(\gamma_t - \overline{\gamma})(\gamma_{t+\tau} - \overline{\gamma})}{\sqrt{\sum_{t=0}^{N-1}(\gamma_t - \overline{\gamma})^2 \sum_{t=0}^{N-1}(\gamma_{t+\tau} - \overline{\gamma})^2}}, \qquad (10)$$

where N is the length of the dataset over which the estimation is performed, and depends on the time coherence of the SNR process. We note that in (10) we are estimating the correlation of the power envelope of the fading process, and therefore remove the average value from the SNR time series [22]. The Nakagami m-parameter can finally be estimated as

$$m = \frac{\overline{\gamma}^2}{\mathbb{E}[(\gamma - \overline{\gamma})^2]}. \qquad (11)$$

The spectral efficiency η must be computed by considering the joint distribution of γ and γ_τ. In particular, in the present analysis, we define η as the spectral efficiency of the chosen modulation whenever the SNR γ_τ (which affects the actual transmission) is sufficient to support the modulation, and 0 otherwise. Therefore, we have

$$\eta = \sum_{j=0}^{J} \tilde{M}_j \int_{\gamma_j^*}^{\gamma_{j+1}^*} \int_{\gamma_j^*}^{+\infty} f_{\gamma_\tau|\gamma}(\gamma_\tau)\, f_\gamma(\gamma)\, \mathrm{d}\gamma_\tau\, \mathrm{d}\gamma \qquad (12)$$

and, similarly to the instantaneous knowledge case, the throughput is found as

$$G = \sum_{j=0}^{J} \tilde{M}_j \int_{\gamma_j^*}^{\gamma_{j+1}^*} \int_{\gamma_j^*}^{+\infty} \left[1 - P_b^{(j)}(\gamma_\tau)\right] f_{\gamma_\tau|\gamma}(\gamma_\tau)\, f_\gamma(\gamma)\, \mathrm{d}\gamma_\tau\, \mathrm{d}\gamma\,. \qquad (13)$$

III. Experimental data set

Our data set is part of the data collected during the SubNet 2009 sea trials, organized by the NATO Undersea Research Centre (NURC) off the eastern shore of the Pianosa Island, Italy (42.585°N, 10.1°E) [23]. The experimental testbed consisted of one vertical array (VA) of three hydrophones moored at 20, 40 and 80 m and denoted in the following as H1, H2, and H3, respectively. Three Teledyne-Low Frequency modems [24] were installed on a tripod on the sea floor, and used as transmitters of custom waveforms. The three transmitters were placed at different distances and depth from the hydrophones: T1 was 1500 m away from the VA at a depth of 60 m, whereas T2 was farther, at 2200 m from the VA, depth 70 m, and T3 closer (700 m from the VA at a depth of 80 m). The environmental conditions of the region were found to be quite stable, with the exception of surface roughness, which greatly varied during the experiment period, due to short wind bursts over 10 m/s. The sound speed profile (SSP) along the watercolumn consistently showed a downward-refractive behavior [23].

The testbed was used to transmit a number of JANUS waveforms at different times of day and under different transmission pattern; while we refer the reader to [25] for a description of the acoustic signal format and purposes, suffice it to say here that the signal contained a detection preamble composed of a probe signal (a chirp or a set of frequency-hopped frequency-shift keying modulation symbols, depending on the signal version), which is used here to obtain SNR traces throughout an experiment starting at 23:30 GMT on 30 August 2010 and lasted until 8:33 GMT on the following day. For reference, we report in Figure 1 an example of SNR time series, for the links between transmitter T1 and all hydrophones, for an experiment lasting almost 9 hours, where transmissions were performed once every 15 s. From this figure we observe a higher SNR on average for the T1–H3 link, which is due to the downward-refractive behavior of the channel; in addition, we observe that in this particular case all links experience time-varying fading effects, as not only do the SNR samples oscillate around their average value, but this average value also varies following changes in propagation conditions (for example, the SNR over T1–H2 steadily increases throughout the experiment).

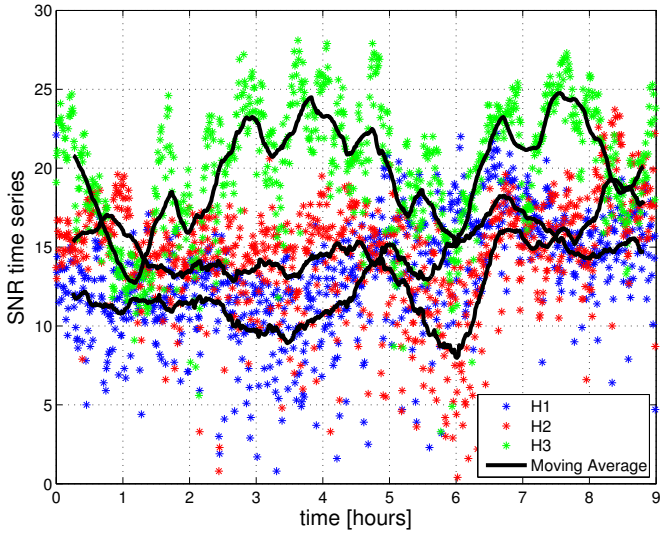

Figure 1. Time series of SNR in dB for transmissions between T1 and all hydrophones during an experiment. Moving averages over 25 samples are provided as a solid black line. The experiment is part of the SubNet'09 program (see also [23]).

The time-varying channel behavior seen in the SubNet 2009 experiments is the main motivation behind the choice to set up a variable-rate modulation scheme for underwater communications, which would allow to exploit the favorable channel conditions, while shielding against excessively poor performance when the SNR drops.

IV. Analysis and simulation results

We start the description of our results by considering spectral efficiency, for the experiment and the links already presented in Figure 1. We focus on this specific subset of results because it shows a highly time-varying channel set; other experiments show either analogous channel conditions, or a more stationary behavior, which is easier for the system to keep track of, and therefore somehow less interesting for the contents of this paper.

Figures 2, 3 and 4 detail the spectral efficiency against average SNR for links from T1 to H1, H2 and H3, respectively.

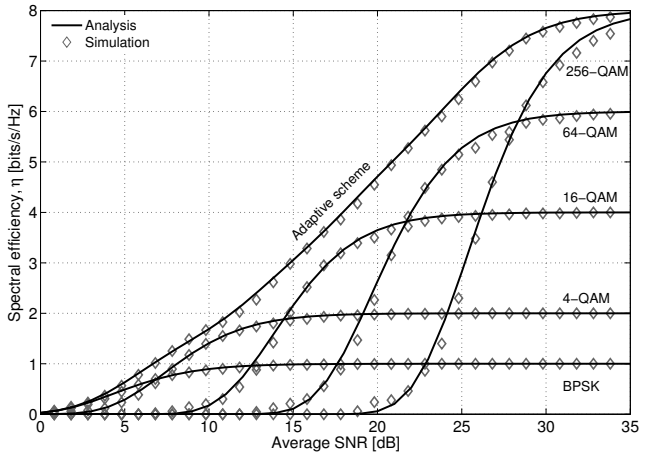

Figure 2. Comparison between theoretic and simulated spectral efficiency vs. SNR over link T1–H1 in the instantaneous knowledge case.

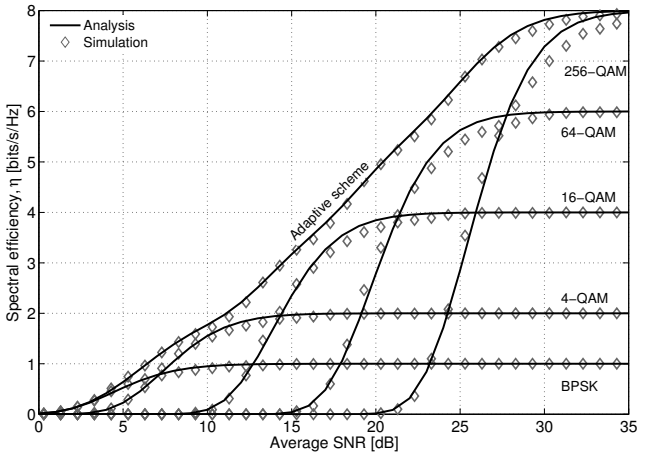

Figure 3. Comparison between theoretic and simulated spectral efficiency vs. SNR over link T1–H2 in the instantaneous knowledge case.

The average SNR is computed by taking the expectation of the SNR time series over the experiment (or a portion thereof), and is varied by adding a constant value: note that this corresponds to simulating a different transmit power than actually employed in the experiments. We consider only instantaneous channel knowledge for the moment. The figures contain both theoretical and simulated curves. In particular, theoretical performance is obtained by estimating the parameters of the correlated Nakagami-m model (in terms of the coefficient m and the correlation ρ) and then using the statistics of the model to obtain performance figures as per the analysis in Section II. On the contrary, simulations take the SNR time series (offset by the same constant value used in the analysis to simulate different transmit power) and reproduce the behavior of the system over that time series. Analytical curves are provided in the figures as solid black lines, whereas simulation results are depicted using grey markers. In order to show that moderate time variations of the SNR statistics do not impact substantially on the results of the estimation, we have chosen a window of 100 minutes in Figure 1, from 2:30 to 4:10 from the beginning of the experiment. In this window, T1–H1's and T1–H2's SNRs are almost constant, whereas T1–H3's experiences more abrupt ups and downs spanning $10\,\mathrm{dB}$ (see Fig. 1). Nevertheless, simulations adhere quite accurately to analysis, in particular for the adaptive scheme. Non-adaptive schemes also show a very good accordance of analysis and simulations. Note that the adaptive scheme does not closely follow the envelope of the non-adaptive ones: this is expected because the SNR is not fixed, but rather follows a Nakagami-m pdf whose mean is reported in the abscissa of the graphs. In the presence of instantaneous channel knowledge, this may allow the use of modulations of larger constellation size, yielding a higher average spectral efficiency than achieved by the best non-adaptive scheme for the same average SNR.

The next metric of interest for our comparison is bit error outage (BEO), which suggests whether the adaptive scheme is successful enough at compensating for changes in the

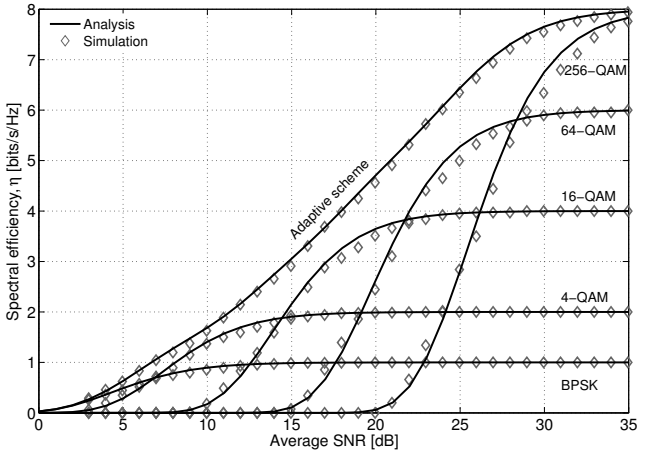

Figure 4. Comparison between theoretic and simulated spectral efficiency vs. SNR over link T1–H3 in the instantaneous knowledge case.

channel by adapting the modulation rate. We remark that, when affected by delayed channel knowledge, adaptation is expected to be less effective, as while channel knowledge is acquired, not only the absolute value, but also the statistics of the channel fading phenomena will have changed. Figures 5 to 7 show the BEO metric for the links from T1 to H1, H2 and H3, respectively. The different behaviors observed in Figure 1 for the channel SNR traces reflect in different outage probability in the figures. We provide both simulated curves and analytical predictions, for both the instantaneous and the delayed channel knowledge cases; for the latter, different delays are provided. The first result is that while the BEO of instantaneous knowledge steadily decreases for increasing SNR, delayed knowledge causes outage events to be likely even for high SNR, creating a sort of floor effect whereby the BEO does not decrease below 0.1 in all figures, until the average SNR is higher than roughly $30\,\mathrm{dB}$. In addition, we observe that more stationary SNR trace chunks (i.e., where the statistics of the SNR do not change much within the

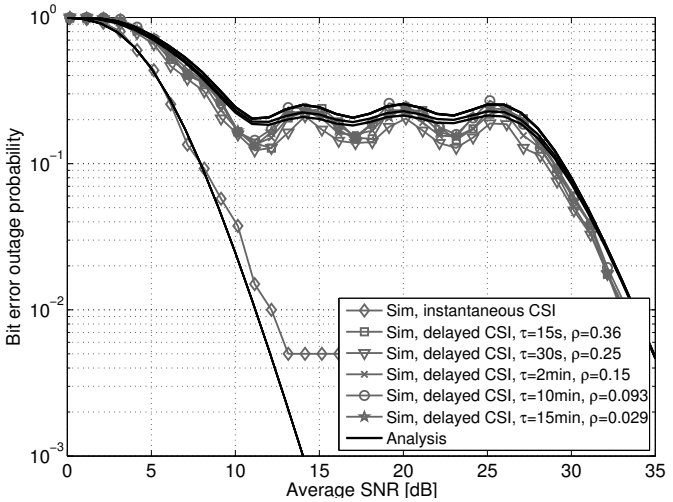

Figure 5. Bit error outage probability as a function of the average SNR for link T1–H1 , $m = 3$.

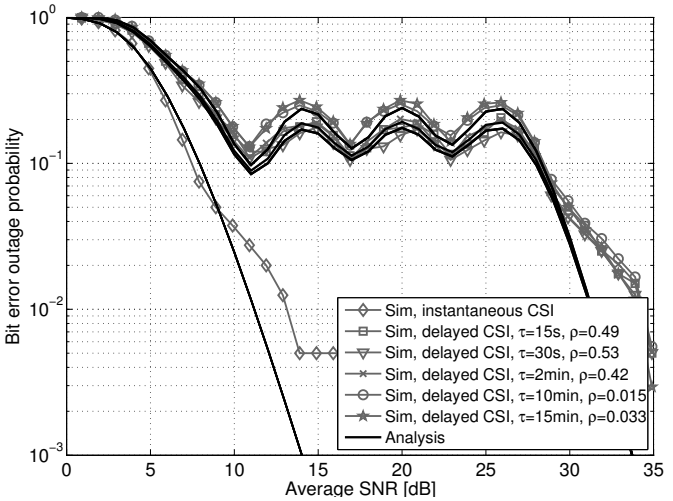

Figure 6. Bit error outage probability as a function of the average SNR for link T1–H2, $m = 5$.

interval where the estimation of the model parameters is performed), do not show substantial difference between the model and simulation results. However, m and ρ are key to a correct prediction, which is by itself inaccurate for two reasons: short windows contain few samples and thus do not allow to correctly estimate the statistics of the signal; longer windows contain enough samples, but may incur state changes in the channel behavior, which would also deviate the estimated channel parameters. For these reasons, the predicted performance in the presence of delayed knowledge correctly estimates the level of the BEO floors, but shows some offset in the oscillations around such floors.

Figures 8(a)–(c) show the average BEO evolution over time for the T1–H1 link. In terms of hours and minutes from the beginning of the experiment, Figure 8(a) refers to the time interval from 0:00 to 1:40, Figure 8(b) to the interval from 3:20 to 5:00 and Figure 8(c) to the interval from 5:00 to 6:40. We observe that the behavior of the channel changes considerably, both in terms of the parameter m of the Nakagami model (impacting BEO oscillations when the SNR ranges from 10 to $30\,\mathrm{dB}$) and in terms of the correlation among samples when delayed channel knowledge versions are considered (impacting the level of the BEO floor before high SNR is reached, as low correlation leads to a higher chance of choosing the wrong modulation.

The last metric we evaluate is the link throughput for the adaptive modulation scheme, G, defined as the spectral efficiency multiplied by the probability of success, averaged over the probability of selecting a specific modulation. Figures 9(a) to 9(b) detail the behavior of the throughput for links from T1 to H1, H2, and H3, respectively. The figures report both the instantaneous and the delayed channel knowledge cases. We observe that the lack of timely knowledge impairs the throughput performance, as a consequence of higher bit error rates (bit error outage is a more likely event). This effect is amplified by greater delays, though as expected the loss of

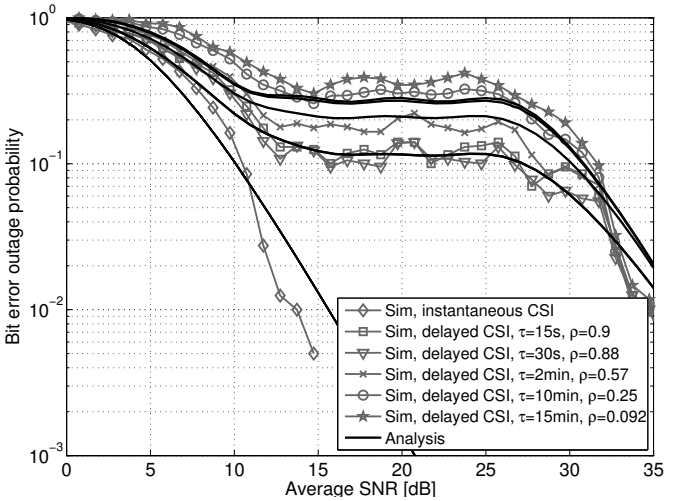

Figure 7. Bit error outage probability as a function of the average SNR for link T1–H3, $m = 2$.

correlation makes high delays equally inconvenient. However, this decrease is still acceptable, especially in stationary scenarios where the correlation is sufficiently high, as is the case for links T1–H1 and T1–H2. We note in fact that all figures refer to the time window in the middle of the experiment, from 4:10 to 5:50 after the beginning. In this phase, we observe a quite stationary behavior over the T1–H1 and T1–H2 links, which results in very good match between analysis and simulation. On the other hand, the T1–H3 link experiences long-term variations of larger amplitude over the considered time window (see Figure 1), which result in a poorer match between analytical and simulated results, especially in case of delayed channel knowledge. However, even in this case, analytical curves are still sufficient to achieve a coarse estimate of the throughput behavior.

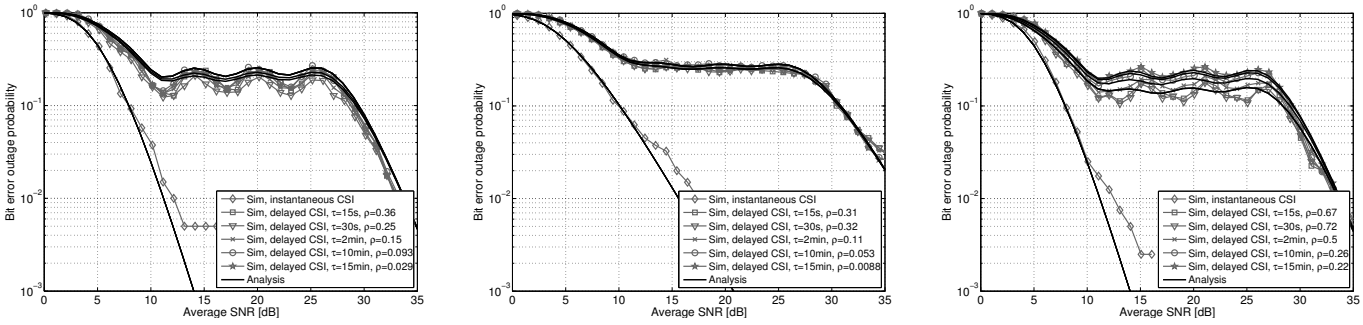

(a) 0:00 to 1:40 (b) 3:20 to 5:00 (c) 5:00 to 6:40

Figure 8. Bit error outage probability as a function of the average SNR for link T1–H1. Analysis and simulation shown for both the instantaneous and the delayed channel knowledge case. For the three links, a value of $m = 3$, $m = 2$ and $m = 3$ is respectively estimated.

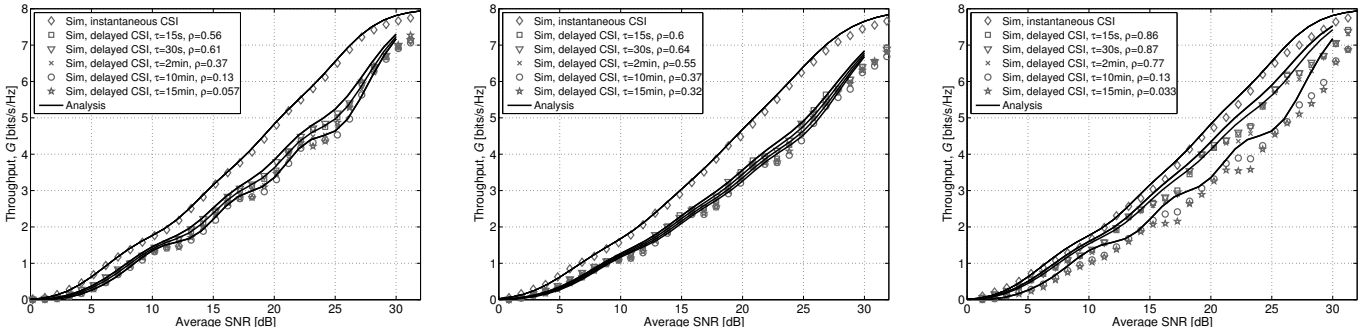

(a) T1–H1 ($m = 3$). (b) T1–H2 ($m = 2$). (c) T1–H3 ($m = 2$).

Figure 9. Throughput as a function of the average SNR for both the instantaneous and the delayed channel knowledge case. For the three links, a value of $m = 3$, $m = 2$ and $m = 2$ is respectively estimated.

V. Conclusions

In this paper, we have employed a correlated Nakagami-m fading model to model the evolution of SNR traces in underwater acoustic channels. This model is found to correctly represent the channel behavior, provided that periods of adequate length are chosen to perform parameter estimation. We have then considered adaptive variable-rate modulation schemes for underwater acoustic networks, and applied the channel model to estimate the performance of such schemes in the presence of both instantaneous and delayed information about the channel model. Results show that whenever the parameter estimation is accurate enough (i.e., when performed over a time window where the fading process is approximately stationary), the model can reproduce the performance of the adaptive modulation scheme as simulated on the channel traces in terms of average spectral efficiency, bit error outage probability and throughput. On the contrary, when the channel experiences fast variations within a given time window, the estimation of such metrics may be less accurate, yet the general behavior of the channel can still be captured, as is the case for bit error outage, whose average value in the delayed channel knowledge case is correctly estimated, although the model may fail to capture minor oscillations around this value.

Future work on this topic involves the study of slow adaptive modulation (SAM), as well as the extension of the analysis to M-QAM modulated OFDM subcarriers, which are more suited to frequency-selective fading, often found in underwater channels.

Acknowledgment

This work has been supported in part by the Italian Institute of Technology (IIT) through the project SEED framework. The authors would like to thank Giovanni Zappa and Kim McCoy, of the NATO Undersea Research Centre, La Spezia, Italy, for their help in obtaining transmission SNR traces from the SubNet'09 experiments.

References

[1] E. M. Sözer and M. Stojanovic, "Reconfigurable acoustic modem for underwater sensor networks," in *Proc. of ACM WUWNet*, Los Angeles, CA, 2006, pp. 101–104.

[2] D. Torres, J. Friedman, T. Schmid, and M. B. Srivastava, "Software-defined underwater acoustic networking platform," in *Proc. of ACM WUWNet*, Berkeley, CA, 2009, pp. 1–8.

[3] P. Qarabaqi and M. Stojanovic, "Statistical modeling of a shallow water acoustic communication channel," in *Proc. of IACM UAM*, Nafplion, Greece, Jun. 2009.

[4] J. Yang, D. Rouseff, D. Tang, and F. S. Henyey, "Effect of the internal tide on acoustic transmission loss at midfrequencies," *IEEE J. Ocean. Eng.*, vol. 35, pp. 3–11, 2010.

[5] M. Stojanovic, "Recent advances in high-speed underwater acoustic communications," *IEEE J. Ocean. Eng.*, vol. 21, no. 2, pp. 125–136, Apr. 1996.

[6] M. Chitre, S. Shahabudeen, and M. Stojanovic, "Underwater acoustic communications and networking: Recent advances and future challenges," *Marine Tech. Soc. Journal*, vol. 42, no. 1, pp. 103–116, spring 2008.

[7] A. Radosevic and J. G. Proakis and M. Stojanovic, "Statistical Characterization and Capacity of Shallow Water Acoustic Channels," in *Proc. of IEEE OCEANS*, Bremen, May 2009.

[8] F. Pignieri, F. De Rango, F. Veltri, S. Marano, "Markovian approach to model underwater acoustic channel: techniques comparison," in *Proc. of IEEE MILCOM*, San Diego, Nov. 2008.

[9] A. J. Goldsmith and S.-G. Chua, "Variable-rate variable-power MQAM for fading channel," *IEEE Trans. Commun.*, vol. 45, no. 10, pp. 1218–1230, Oct. 1997.

[10] S. Zhou and G. B. Giannakis, "How accurate channel prediction needs to be for transmit-beamforming with adaptive modulation over Rayleigh MIMO channels?" *IEEE Trans. on Wireless Commun.*, vol. 3, no. 4, pp. 1285–1294, Jul. 2004.

[11] T. Keller and L. Hanzo, "Adaptive modulation techniques for duplex OFDM transmission," *IEEE Trans. on Veh. Technol.*, vol. 49, no. 5, pp. 1893–1906, Sep. 2000.

[12] N. Baldo, F. Maguolo, S. Merlin, A. Zanella, M. Zorzi, D. Melpignano, and D. Siorpaes, "APOS: Adaptive Parameters Optimization Scheme for voice over IEEE 802.11g," in *Proc. of IEEE ICC*, Beijing, China, May 2008, pp. 2466–2472.

[13] J. A. Rice, V. K. McDonald, M. D. Green, and D. Porta, "Adaptive modulation for undersea acoustic telemetry," *Sea Technology*, vol. 40, no. 5, pp. 29–36, May 1999.

[14] X. Yu, "Wireline quality underwater wireless communication using high speed acoustic modems," in *Proc. of MTS/IEEE OCEANS*, vol. 1, Providence, RI, Sep. 2000, pp. 417–422.

[15] S. Mani, T. M. Duman, and P. Hursky, "Wireline quality underwater wireless communication using high speed acoustic modems," in *Proc. of Acoustics'08*, Paris, France, Jun. 2008, pp. 4255–4260.

[16] European Telecommunications Standards Institute, "Digital Video Broadcasting standards." [Online]. Available: http://www.etsi.org/website/technologies/dvb.aspx

[17] W. Webb and R. Steele, "Variable rate QAM for mobile radio," *IEEE Trans. Commun.*, vol. 43, no. 7, pp. 2223–2230, Jul. 1995.

[18] K. Cho and D. Yoon, "On the general BER expression of one- and two-dimensional amplitude modulations," *IEEE Trans. Commun.*, vol. 50, no. 7, pp. 1074–1080, Jul. 2002.

[19] M. K. Simon and M.-S. Alouini, *Digital Communication over Fading Channels: A Unified Approach to Performance Analysis*, 1st ed. New York, NY: John Wiley & Sons, Inc., 2000.

[20] M.-S. Alouini and A. J. Goldsmith, "Adaptive modulation over Nakagami fading channels," *Wireless Personal Communications Journal*, vol. 13, no. 1-2, pp. 119–143, May 2000.

[21] I. Gradshteyn and I. M. Ryzhik, *Table of Integrals, Series and Products*. Academic Press, 1980.

[22] J. Wallace, H. Ozcelik, M. Herdin, E. Bonek, and M. Jensen, "Power and complex envelope correlation for modeling measured indoor MIMO channels: a beamforming evaluation," in *Proc. of IEEE VTC-Fall*, vol. 1, Orlando, FL, Oct. 2003, pp. 363–367.

[23] B. Tomasi, G. Zappa, K. McCoy, P. Casari, and M. Zorzi, "Experimental study of the space-time properties of acoustic channels for underwater communications," in *Proc. IEEE/OES Oceans*, Sydney, Australia, May 2010.

[24] "Teledyne benthos undersea systems and equipment," www.benthos.com.

[25] K. McCoy, "JANUS: from primitive signal to orthodox networks," in *Proc. of IACM UAM*, Nafplion, Greece, Jun. 2009.